Supporting Information

Zhang et al. 10.1073/pnas.1203280109

SI Materials and Methods

Cell Culture and E2 Treatments. MCF-7 cells were maintained in DMEM supplemented with 10% calf serum. The PAD2-depleted MCF-7 cell line was generated by transfection of MCF-7 cells with a Mission shRNA Plasmid DNA containing a short hairpin RNA (shRNA) construct targeting the human PAD2 coding sequence (Sigma; SHCLND-NM_007365) using FuGENE6 (Roche). The stable PAD4-depleted MCF-7 cell line was described (1). In the control group, cells were transfected with a nontargeting shRNA control vector (Sigma SHC002). Cells were selected by medium containing 1 μg/mL puromycin (Sigma). Flag-tagged PAD2 overexpression MCF-7 cells were generated by transfection with Flag-PAD2-pcDNA3.1 (+) and selected by medium containing 0.5 μg/mL puromycin. HeLa-ER cells were kindly provided by W. Lee Kraus (University of Texas Southwestern Medical Center, Dallas, TX). HeLa, HeLa-ER, and MDA-MB231 cells were maintained in DMEM supplemented with 10% (vol/vol) FBS. Before E2 treatment, the cells were cultured for 3 d in DMEM phenol red-free medium supplemented with 10% (vol/vol) charcoal-dextran–treated calf serum. ICI182780 was used at 10 μM for 18 h before the addition of E2.

Mouse Ovariectomy (OVX), E2 Treatment, and Immunohistochemistry (IHC). Female nu/nu nude mice (4-wk-old; The Jackson Laboratory) were ovariectomized and simultaneously implanted with s.c. estrogen pellets (0.72 mg per pellet, 60-d release; Innovative Research of America) or a sham control pellet ($n = 3$ per group). The mice were killed 3 wk after treatment. Uterine tissue was excised, fixed in 10% buffered formalin, embedded in paraffin, sectioned, and stained with anti-H3Cit26 antibody (Abcam; ab19847, lot 135757).

Confocal Microscopy. Cells grown on slides were subjected to E2 treatment for 45 min. Confocal microscopy experiments were described (2). Antibody used were as follows: anti-H3Cit26 (Abcam; ab19847, lot 135757), anti-H3Cit2/8/17 (Abcam; ab77164), H4Cit3 (Millipore; 07–596), Ac-H4K5 (Abcam; ab51997), H3K9 dimethyl (Abcam; ab1220), H3K27 trimethyl (Abcam; ab6002), and ERα (Abcam; ab2746). Images were collected with LSM 510 laser scanning confocal microscope (Carl Zeiss).

Chromatin Immunoprecipitation (ChIP) and ChIP-chip. ChIP experiments were performed as described (1). Estrogen was used at concentration of 100 nM for 45 min, Antibodies used were anti-H3Cit26 (Abcam; ab19847, lot 135757), anti-ERα (Santa Cruz; sc-542), and anti-Flag (Sigma; F3165). Primers used for the ChIP-qPCR were listed as below. ChIP for H3Cit26 coupled with hybridization to a human HG18 RefSeq promoter microarray from Nimblegen, and genomic data analyses were performed as described (1). The $\log_2$ ratio (IP/Input) data from each array was subjected to Lowess normalization (3). The normalized data were scaled to equivalent sum of squares and then the between-array mean $\log_2$ ratio was determined for each probe. An error model was generated by using a 1-kb moving window with 250-bp steps in which both the mean probe $\log_2$ ratio and P values were calculated for each window. The P values were calculated by using the nonparametric Wilcoxon signed-rank test. Significant peaks were defined as the center of three consecutive windows with positive means, the center window with a mean greater than either adjacent window, and all windows having significant P value less than 0.016. Induced regions were defined as H3Cit26-bound regions (present in the E2-treated samples) that had both a significant P value and a fold ratio >1.148 compared with the EtOH samples. Reduced regions were defined as H3Cit26-bound regions (present in the EtOH control samples) that had both a significant P value and a fold <1 compared with the E2-treated samples. Constitutive regions were defined as H3Cit26-bound regions (present in both conditions) that did not have a significant P value form the composite fold analysis. The TSS-anchored ChIP-chip heat maps were generated by using 600-bp windows with 150-bp steps and were visualized with Java Treeview (4). The data can be accessed through the NCBI/GEO website by using accession number GSE32599.

Steady-State Kinetic Assays. PAD2 was purified by established methods (5, 6). PAD4 was purified as described (7). Histone-based peptides were synthesized by using the Fmoc approach and purified by reverse-phase HPLC to ≥95%. Kinetic assays were performed as described (8). Briefly, reaction buffer (100 mM Tris·HCl at pH 7.6, 2 mM DTT, 10 mM CaCl2, and 50 mM NaCl) was preincubated for 10 min at 37 °C with varying concentrations of histone H3 (0–180 μM), or peptide (22–30) (0–10 mM). The reaction was initiated by the addition of enzyme (0.2 μM final). After 6 min, reactions were quenched by flash freezing in liquid nitrogen, and 200 μL of COLDER solution was added to each tube. The absorbance at 540 nm was quantified and product formation determined by comparing the absorbance to a citrulline standard curve. The data were fit to the following equation: $v = V_{max}[S]/(K_m+[S])$ by using the GraFit version 5.0.11 software package (9).

Acid Extraction of Histones, PAD Assay, and Western Blotting. MCF-7 cells were first E2 starved, followed by 100 nM E2 treatment for 45 min. EtOH treatment was used as a control. Cellular histones were purified by acid extraction (2). For the PAD assay, human PAD2 proteins were expressed and purified from pET16-PAD2 by using Ni-NTA Protein Purification System (Qiagen). The PAD assay was performed as described (2). Histone samples were separated by 15% SDS/PAGE, and the membrane was detected by Western blot using anti-H3Cit26 (ab19847, lot 135757), and anti-H3 (Abcam; ab1791).

Identification of Arg26 Citrullination in Human Histone H3 by nanoLC/MS/MS Analysis Using LTQ Orbitrap Velos. The PAD2-treated H3 bands were excised from gel and subjected to digestion and extraction as reported (10). The digest was reconstituted in 10 μL of 2% acetonitrile (ACN) with 0.5% formic acid (FA) for nanoLC-ESI-MS/MS analysis, which is carried out by using a LTQ-Orbitrap Velos (Thermo-Fisher Scientific) mass spectrometer equipped with "Plug and Play" nano ion source device (CorSolutions). The nanoLC was carried out by Dionex UltiMate3000 MDLC system (Dionex). The tryptic peptides (5–10 μL) was injected onto a PepMap C18 trap column at 20 μL/min flow rate and then separated on a PepMap C18 RP nano column, which was installed in the Plug and Play device with a 10-μm spray emitter (New Objective) mounted in front of Orbitrap orifice. The peptides were then eluted in a 90-min gradient of 10–40% ACN in 0.1% FA at 300 nL/min, followed by a 3-min ramping to 95% ACN-0.1% FA and a 5-min holding at 95% ACN-0.1% FA. The column was reequilibrated with 2% ACN-0.1% FA for 20 min before the next run. The Orbitrap Velos was operated in positive ion mode with nanospray voltage set at 1.5 kV and source temperature at 275 °C. Either internal calibration using the background polysiloxane ion signal at m/z 445.120025

as a lock mass or external calibration using Ultramark 1621 for Fourier Transform (FT) mass analyzer was performed. The instrument was performed in parallel data-dependent acquisition (DDA) mode by using FT mass analyzer for one survey MS scan for precursor ions followed by MS/MS scans on the top seven most intensity peaks with multiple charged ions above a threshold ion count of 7,500 in both LTQ mass analyzer and HCD-based FT mass analyzer at 7,500 resolution. MS survey scans at a resolution of 60,000 (FWHM at m/z 400), for the mass range of m/z 375–1800. Dynamic exclusion parameters were set at repeat count 1 with a 20-s repeat duration, exclusion list size of 500, 30-s exclusion duration, and ±10 ppm exclusion mass width. Collision induced dissociation (CID) parameters were set at the following values: isolation width 2.0 m/z, normalized collision energy 35%, activation Q at 0.25, and activation time 10 ms. The activation time is 0.1 ms for HCD analysis. All data are acquired under Xcalibur 2.1 operation software (Thermo-Fisher Scientific). All MS and MS/MS raw spectra were processed and searched by using Proteome Discoverer 1.2 (Thermo-Fisher Scientific) against Human RefSeq database downloaded from NCBInr database. The database search was performed with three-missed cleavage site by trypsin allowed. The peptide tolerance was set to 10 ppm, and MS/MS tolerance was set to 0.8 Da for CID and 0.05 Da for HCD. A fixed carbamidomethyl modification of cysteine, variable modifications on methionine oxidation, asparagine/glutamine deamidation, lysine acetylation/methylation, and arginine citrullination were set. The peptides with low confident score (with Xcorr score <2 for doubly charged ion and <2.7 for triply charged ion) defined by PD1.2 were filtered out, and the remaining peptides were considered for the peptide identification with possible modification determinations. All MS/MS spectra for possibly modified peptides identified from initial database searching were manually inspected and validated by using both PD1.2 and Xcalibur 2.1 software.

Immunoprecipitation Assay. MCF-7 cells and MCF-7 cells stably overexpressing Flag-tagged PAD2 were estrogen starved for 3 d followed by 100 nM E2 stimulation for 45 min at 37 °C. The whole-cell lysates were immunoprecipitated with anti-ER or anti-Flag M2 affinity gel (Sigma; A2220). Immunoprecipitates were analyzed by Western blot using anti-PAD2 (ProteinTech; 122100-1-AP), anti-ERα, and anti-Flag antibodies as indicated. The overexpression of Flag-PAD2 was verified by Western blot with anti-Flag and anti–β-actin (Sigma; A2066) antibodies.

Primers for ChIP-qPCR, RT-qPCR, and MNase Protection-qPCR.

ChIP-qPCR:
- TFF1 TSS1670-Fwd 5′-CCCACCTTTTCTCCAAATGA-3′
- TFF1 TSS1670-Rev 5′-GGTGGTTTTCGCTGCTCTAA-3′
- TFF1 TSS1339-Fwd 5′-AGAGGGGCTGCAGAAATGTA-3′
- TFF1 TSS1339-Rev 5′-GCTGCATGAAGAAATGGACA-3′
- TFF1 TSS1167-Fwd 5′-GCCACTGTTCTAGGGTCTGG-3′
- TFF1 TSS1167-Rev 5′-TGGGAGCAGAAGTCCTCATC-3′
- TFF1 TSS959-Fwd 5′-GAGCAGGAGGCTGTCCTCTA-3′
- TFF1 TSS959-Rev 5′-GTGGTTCACTCCCCTGTGTC-3′
- TFF1 TSS357-Fwd 5′-TTCCGGCCATCTCTCACTAT-3′
- TFF1 TSS357-Rev 5′-ATGGGAGTCTCCTCCAACCT-3′
- TFF1 TSS273-Fwd 5′-CCTGGATTAAGGTCAGGTTGGA-3′
- TFF1 TSS273-Rev 5′- TCTTGGCTGAGGGATCTGAGA-3′
- TFF1 TSS205-Fwd 5′- AGCCAAGATGACCTCACCAC-3′
- TFF1 TSS205-Rev 5′- TGGTCAAGCTACATGGAAGG-3′
- TFF1 TSS160-Fwd 5′- TTGTGGTTTTCCTGGTGTCA-3′
- TFF1 TSS160-Rev 5′- ACAGCAGCCCTTATTTGCAC-3′
- KRT13 TSS 1041-Fwd 5′-GTTACACCAGGGGTGTGGAG-3′
- KRT13 TSS 1041-Rev 5′-TTCCCAGCATTCCATAAAGG-3′
- KRT13 TSS 662-Fwd 5′-ACAGGGCCACTTCCTCTTTC-3′
- KRT13 TSS 662-Rev 5′-TTAGGGACCATCAGACACAGC-3′
- KRT13 TSS 620-Fwd 5′-TGTCTGATGGTCCCTAAGATCC-3′
- KRT13 TSS 620-Rev 5′-CGAGGCCATCAGAAAAAGTC-3′
- SCN1A TSS1083-Fwd 5′-CAAATAAAATTCATGGCCAAGTG-3′
- SCN1A TSS1083-Rev 5′-GCCAAAATATTCCAGAGCCTAA-3′
- SCN1A TSS823-Fwd 5′-TTGAGTTTATGGCACCCTGAC-3′
- SCN1A TSS823-Rev 5′-GTGCAGGAGACAGCAGGAGT-3′

RT-qPCR:
- TFF1-Fwd 5′-CATCGACGTCCCTCCAGAAGAG-3′
- TFF1-Rev 5′-CTCTGGGACTAATCACCGTGCTG-3′
- KRT13-Fwd 5′-GGCAGAGATGAGGGAGCAGTA-3′
- KRT13-Rev 5′-TCTTGGCGTGGAACCATTC-3′
- GREB1-Fwd 5′-CAAAGAATAACCTGTTGGCCCTGC-3′
- GREB1-Rev 5′-GACATGCCTGCGCTCTCATACTTA-3′
- CYP1B1-Fwd 5′-AACGTACCGGCCACTATC-3′
- CYP1B1-Rev 5′-CACGACCTGATCCAATTC-3′
- WISP2-Fwd 5′-GAGAGGCACACCGAAGAC-3′
- WISP2-Rev 5′-GGCAGGTACATGGTGTCG-3′
- SCN1A-Fwd 5′-CCTACATCGCCTGTTGGAC-3′
- SCN1A-Rev 5′-CCATGGAAACGTGGAAAGAA-3′
- VAT1L-Fwd 5′-CAAGAGCTTCTTCAGCTTTGC-3′
- VAT1L-Rev 5′-TTGATGGGGTTCACCTTCTC-3′
- ACTB-Fwd 5′-CCAACCGCGAGAAGATGA-3′
- ACTB-Rev 5′-CCAGAGGCGTACAGGGATAG-3′
- GAPDH-Fwd 5′-AGCCACATCGCTCAGACAC-3′
- GAPDH-Rev 5′-GCCCAATACGACCAAATCC-3′

MNase protection-qPCR:
- TFF1a-Fwd 5′-GCTTAGGCCTAGACGGAATG-3′
- TFF1a-Rev 5′-TGACCTTGCAGGGGGAAG-3′
- TFF1b-Fwd 5′-TTCATGAGCTCCTTCCCTTC-3′
- TFF1b-Rev 5′-GTGACAACAGTGGCTCACG-3′
- TFF1c-Fwd 5′-CCCGTGAGCCACTGTTGT-3′
- TFF1c-Rev 5′-TAGTGAGAGATGGCCGGAAA-3′
- TFF1d-Fwd 5′-TTCCGGCCATCTCTCACTAT-3′
- TFF1d-Rev 5′-CCCGCCAGGGTAAATACTGT-3′
- TFF1e-Fwd 5′-CGGGAGGGCCTCTCAGATA-3′
- TFF1e-Rev 5′-ATGGGAGTCTCCTCCAACCT-3′
- TFF1f-Fwd 5′-AAGGTCAGGTTGGAGGAGAC-3′
- TFF1f-Rev 5′-TGAGGGATCTGAGATTCAGAAAG-3′
- TFF1g-Fwd 5′-TCAGATCCCTCAGCCAAGAT-3′
- TFF1g-Rev 5′-TGGAAGGATTTGCTGATAGACA-3′
- TFF1h-Fwd 5′-TCACCACATGTCGTCTCTGTC-3′
- TFF1h-Rev 5′-TGGTCAAGCTACATGGAAGG-3′
- TFF1i-Fwd 5′-GCTTGACCATGTCTAGGAAACA-3′
- TFF1i-Rev 5′-CGGGGATCCTCTGAGACA-3′
- TFF1j-Fwd 5′-CAGTGGAGATTATTGTCTCAGAGG-3′
- TFF1j-Rev 5′-CGTTAGATAACATTTGCCTAAGGA-3′
- TFF1k-Fwd 5′-GGCCTCCTTAGGCAAATGTT-3′
- TFF1k-Rev 5′-AGCCCCGGATTTTATAGGG-3′
- KRT13a-Fwd 5′-TCAGTCCTGATTCTGCCCTTA-3′
- KRT13a-Rev 5′-CCACAGGAGGAGGGTCCTA-3′
- KRT13b-Fwd 5′-CATGTGTAAATGGGGGCAAT-3′
- KRT13b-Rev 5′-AGGCAGGAACTGGGTGAAGT-3′
- KRT13c-Fwd 5′-CTTCACCCAGTTCCTGCCTA-3′
- KRT13c-Rev 5′-AGTGGCCCTGTCCATTATCA-3′
- KRT13d-Fwd 5′-ACAGGGCCACTTCCTCTTTC-3′
- KRT13d-Rev 5′-TTAGGGACCATCAGACACAGC-3′
- KRT13e-Fwd 5′-TGTCTGATGGTCCCTAAGATCC-3′
- KRT13e-Rev 5′-CGAGGCCATCAGAAAAAGTC-3′
- KRT13f-Fwd 5′-GGCCTCGGAGCTATTTCTTT-3′
- KRT13f-Rev 5′-CGATAGAATCACCTGCCTTGA-3′
- KRT13g-Fwd 5′-TCAAGGCAGGTGATTCTATCG-3′
- KRT13g-Rev 5′-GGGATGTCCTGGATCCTTCT-3′

KRT13h-Fwd 5′-GGCCCCTGGAGTAGATGAAG-3′
KRT13h-Rev 5′-CTGACTGGGATGTCCTGGAT-3′
KRT13i-Fwd 5′-ATCCAGGACATCCCAGTCAG-3′
KRT13i-Rev 5′-CAGAGTGGCTCTGTGCTTTG-3′
KRT13j-Fwd 5′-ACTCTGCACCCACCACTTTC-3′
KRT13j-Rev 5′-AGAACGGGACCTGAGATGC-3′
WISP2a-Fwd 5′- GGCACCTCCATCAGAAAGTG-3′
WISP2a-Rev 5′- TTCAGGAATACCAGGCAAGG-3′
WISP2b-Fwd 5′- GGTATTCCTGAACTTCCACCTG -3′
WISP2b-Rev 5′- GAGGCACAACACTGACCTGA-3′
WISP2c-Fwd 5′- TCCTCAGGTCAGTGTTGTGC -3′
WISP2c-Rev 5′- GATGGGGTCAAGCCAAATC-3′
WISP2d-Fwd 5′- CAAATGGATTTGGCTTGACC -3′
WISP2d-Rev 5′- GGCAGGCTGGACCTACTATG-3′
WISP2e-Fwd 5′- CAAGCGCTGGCACATAGT -3′
WISP2e-Rev 5′- ATAAGGGGCCTCCCTTGG-3′
WISP2f-Fwd 5′- CCCTTATTGCCAAGAGCAAAC -3′
WISP2f-Rev 5′- TGACCCAGAGCAAAACTTCC-3′
WISP2g-Fwd 5′- GGAAGTTTTGCTCTGGGTCA -3′
WISP2g-Rev 5′- GGTTTCTGGCAGGCAGATT-3′
WISP2h-Fwd 5′- AATCTGCCTGCCAGAAACC -3′
WISP2h-Rev 5′- GTGGCCCTGACTCTGGGTAG-3′
WISP2i-Fwd 5′- CCACGGAGCTTAGGAGACCT -3′
WISP2i-Rev 5′- CAGTAAACAACCCCTTTGCAG-3′
WISP2j-Fwd 5′- AGCTCTGCAAAGGGGTTGTT -3′
WISP2j-Rev 5′- CCTATTCCAGACCCCCTGTC-3′
WISP2k-Fwd 5′- GACAGGGGGTCTGGAATAGG -3′
WISP2k-Rev 5′- AGGGTCCTAGCCCTGCTGTA-3′
GREB1a-Fwd 5′- GGAAACAGATGGGAAAGACAA-3′
GREB1a-Rev 5′- CCTCGCTCCAAGACCAGA-3′
GREB1b-Fwd 5′- CCTAGGAGCTCTGGTCTTGG -3′
GREB1b-Rev 5′- TGGCCACAATTGAACATAGG-3′
GREB1c-Fwd 5′- TGTTCAATTGTGGCCAATAAA -3′
GREB1c-Rev 5′- CAAGCCCTGATCAAGGAAAC-3′
GREB1d-Fwd 5′- GTTTCCTTGATCAGGGCTTG -3′
GREB1d-Rev 5′- TTTGCTCAAAGTGAGGACGTT-3′
GREB1e-Fwd 5′- TCCTCACTTTGAGCAAAAGC -3′
GREB1e-Rev 5′- AACAAAAACTAAAGGCGTAAGGA-3′
GREB1f-Fwd 5′- CGCCTTTAGTTTTTGTTTAAAGGT -3′
GREB1f-Rev 5′- ATGACCCAGTTGCCACACTT-3′
GREB1g-Fwd 5′- AGTGTGGCAACTGGGTCATT -3′
GREB1g-Rev 5′- GCTGCGGCAATCAGAAGTAT-3′
GREB1h-Fwd 5′- CCGCAGCAGACAATGATG -3′
GREB1h-Rev 5′- TGAAAAGGCAGCAAACTTGT-3′
GREB1i-Fwd 5′- CTTTTCATTTCTGTGGGTCGT -3′
GREB1i-Rev 5′- ACAGACCCAAACATGCTGCT-3′
GREB1j-Fwd 5′- AGCAGCATGTTTGGGTCTGT -3′
GREB1j-Rev 5′- CTAGTGGGGACAAGCACACA-3′
GREB1k-Fwd 5′- GTGTGTGCTTGTCCCCACTA -3′
GREB1k-Rev 5′- TGGACAAGCCATATCCCTAA-3′
CYP1B1a-Fwd 5′- GCCGCAAGAACTGGAAAA -3′
CYP1B1a-Rev 5′- ACCTCAGTGGAGGCTCTTTG-3′
CYP1B1b-Fwd 5′- CTCCACTGAGGTGGCAATTT -3′
CYP1B1b-Rev 5′- GCCCCTGGTTGGTTGTTTA-3′
CYP1B1c-Fwd 5′- GCTGCCACTACACTGGCTTT -3′
CYP1B1c-Rev 5′- ACGACCTCCCTTCCCTCTC-3′
CYP1B1d-Fwd 5′- GGAGAGGGAAGGGAGGTC -3′
CYP1B1d-Rev 5′- CCACGCTCGGTACAACCT-3′
CYP1B1e-Fwd 5′- GTTGTACCGAGCGTGGTTCT -3′
CYP1B1e-Rev 5′- ACGTTTCCATTGTGCGGTA-3′
CYP1B1f-Fwd 5′- GTTACCGCACAATGGAAACG -3′
CYP1B1f-Rev 5′- GCTCTACCAGCAGGCTTTCA-3′
CYP1B1g-Fwd 5′- ACCTCCGCTCCCATGAAA -3′
CYP1B1g-Rev 5′- ACACCAGGCCGCTTTGAC-3′
CYP1B1h-Fwd 5′- GTCAAAGCGGCCTGGTGT -3′
CYP1B1h-Rev 5′- TCCTCCGGGTTTTAAGGACT-3′
CYP1B1i-Fwd 5′- CCTCCTTCTACCCAGTCCTTAAA -3′
CYP1B1i-Rev 5′- TCCCACTCCCACTCCAGA-3′
CYP1B1j-Fwd 5′- TGACTCTGGAGTGGGAGTGG -3′
CYP1B1j-Rev 5′- CTCACAACTGGAGTCGCAGA-3′
SCN1Aa-Fwd 5′-CAAATAAAATTCATGGCCAAGTG-3′
SCN1Aa-Rev 5′-GCCAAAATATTCCAGAGCCTAA-3′
SCN1Ab-Fwd 5′-TCTGGAATATTTTGGCTCAGTAAT-3′
SCN1Ab-Rev 5′-GACGCCAAATCCCAAATGTA-3′
SCN1Ac-Fwd 5′-ACATTTGGGATTTGGCGTCT-3′
SCN1Ac-Rev 5′-AAAACCGTCAACCCCATACA-3′
SCN1Ad-Fwd 5′-TGTATGGGGTTGACGGTTTT-3′
SCN1Ad-Rev 5′-TGAAATTCTTGCTGATTCTATAGTCC-3′
SCN1Ae-Fwd 5′-CAAGAATTTCATTATTGCTTCAGTG-3′
SCN1Ae-Rev 5′-TCAGGGTGCCATAAACTCAA-3′
SCN1Af-Fwd 5′-TTGAGTTTATGGCACCCTGAC-3′
SCN1Af-Rev 5′-GTGCAGGAGACAGCAGGAGT-3′
SCN1Ag-Fwd 5′-GAGACTCCTGCTGTCTCCTG-3′
SCN1Ag-Rev 5′-GGTGGGGGTGGAAGAAGATA-3′
SCN1Ah-Fwd 5′-ATCTTCTTCCACCCCCACCT-3′
SCN1Ah-Rev 5′-GAAGGAGAGGAAAACTAGGCTGT-3′
SCN1Ai-Fwd 5′-CAGCCTAGTTTTCCTCTCCTTC-3′
SCN1Ai-Rev 5′-AGTCCACGGTTGGACAAATG-3′
SCN1Aj-Fwd 5′-GTCCAACCGTGGACTGTCTT-3′
SCN1Aj-Rev 5′-TGTCCTGCTCACTTCACTAGC-3′
VAT1La-Fwd 5′-GGGCATTTAAAGCAGTGAGG-3′
VAT1La-Rev 5′-AAGTGCTGCCTCTTCTCTCC-3′
VAT1Lb-Fwd 5′-GGGAGAGAAGAGGCAGCACT-3′
VAT1Lb-Rev 5′-TCAGAGCATGAGGCATGAAG-3′
VAT1Lc-Fwd 5′-ACTGTGTCCTTCATGCCTCA-3′
VAT1Lc-Rev 5′-TGGGGTGGACATGATTTCAG-3′
VAT1Ld-Fwd 5′-TGTCTCACTGAAATCATGTCCA-3′
VAT1Ld-Rev 5′-TTTTTCTATATTGTGTGAAGTGCTG-3′
VAT1Le-Fwd 5′-ACCCCAGCACTTCACACAAT-3′
VAT1Le-Rev 5′-CCTGAGCCTCAACACACTCA-3′
VAT1Lf-Fwd 5′-TGTTGAGGCTCAGGAAGGTT-3′
VAT1Lf-Rev 5′-TGCAGGTGAGGAAGTAGGTCT-3′
VAT1Lg-Fwd 5′-CCTCACCTGCATCTCTTTCC-3′
VAT1Lg-Rev 5′-GGAAGGACGTGGTTTTCCTA-3′
VAT1Lh-Fwd 5′-ACTGCCCCTAGGAAAACCAC-3′
VAT1Lh-Rev 5′-GGCTCTTTGAGAAAAACAGCTC-3′
VAT1Li-Fwd 5′-CTGTTTTTCTCAAAGAGCCTGA-3′
VAT1Li-Rev 5′-TGCATGCACATACACAGAGTAG-3′
VAT1Lj-Fwd 5′-TGTATGTGCATGCATGTTGG-3′
VAT1Lj-Rev 5′-GTGTTCTGATCCCCGGAAG-3′
VAT1Lk-Fwd 5′-GAGCGGGTACACACTGGTCT-3′
VAT1Lk-Rev 5′-CACCATTTCGGGCTATTAAAGA-3′

1. Zhang X, et al. (2011) Genome-wide analysis reveals PADI4 cooperates with Elk-1 to activate c-Fos expression in breast cancer cells. *PLoS Genet* 7:e1002112.
2. Wang Y, et al. (2004) Human PAD4 regulates histone arginine methylation levels via demethylimination. *Science* 306:279–283.
3. Smyth GK, Speed T (2003) Normalization of cDNA microarray data. *Methods* 31: 265–273.
4. Saldanha AJ (2004) Java Treeview—extensible visualization of microarray data. *Bioinformatics* 20:3246–3248.
5. Knuckley B, et al. (2010) Substrate specificity and kinetic studies of PADs 1, 3, and 4 identify potent and selective inhibitors of protein arginine deiminase 3. *Biochemistry* 49:4852–4863.
6. Raijmakers R, et al. (2007) Methylation of arginine residues interferes with citrullination by peptidylarginine deiminases in vitro. *J Mol Biol* 367:1118–1129.
7. Knuckley B, Bhatia M, Thompson PR (2007) Protein arginine deiminase 4: Evidence for a reverse protonation mechanism. *Biochemistry* 46:6578–6587.
8. Kearney PL, et al. (2005) Kinetic characterization of protein arginine deiminase 4: a transcriptional corepressor implicated in the onset and progression of rheumatoid arthritis. *Biochemistry* 44:10570–10582.
9. Leatherbarrow RJ (2004) *Grafit Ver 5.0* (Erathicus Software, Staines, UK).
10. Zhang S, Van Pelt CK, Henion JD (2003) Automated chip-based nanoelectrospray-mass spectrometry for rapid identification of proteins separated by two-dimensional gel electrophoresis. *Electrophoresis* 24:3620–3632.

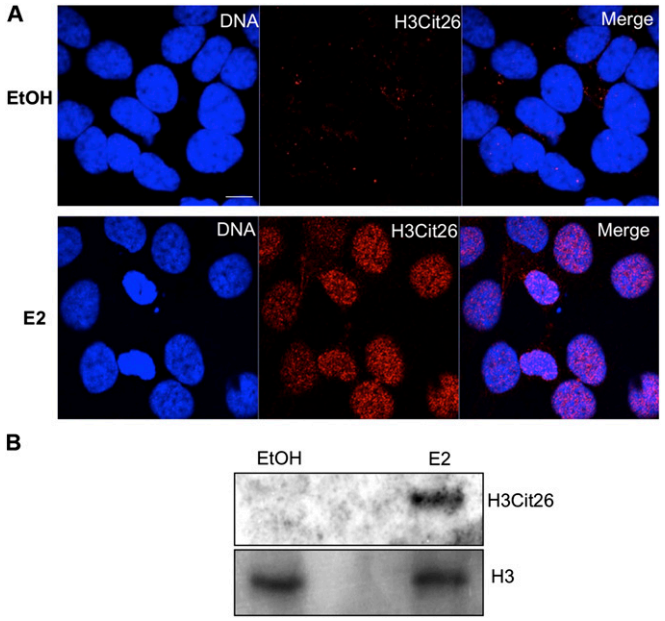

Fig. S1. E2 induced global activation of H3R26 citrullination in MCF-7 cells. (*A*) In the absence of E2 treatment (EtOH control), H3Cit26 signals (red) are very weak. After 45 min of E2 treatment, elevated levels of nuclear H3R26 citrullination are observed. (Scale bar: 10 μm.) (*B*) Western blot showing that amounts of H3Cit26 were increased in MCF-7 cells after E2 treatment. Blotting with anti-Histone H3 (*Lower*) revealed that histone levels between groups were similar.

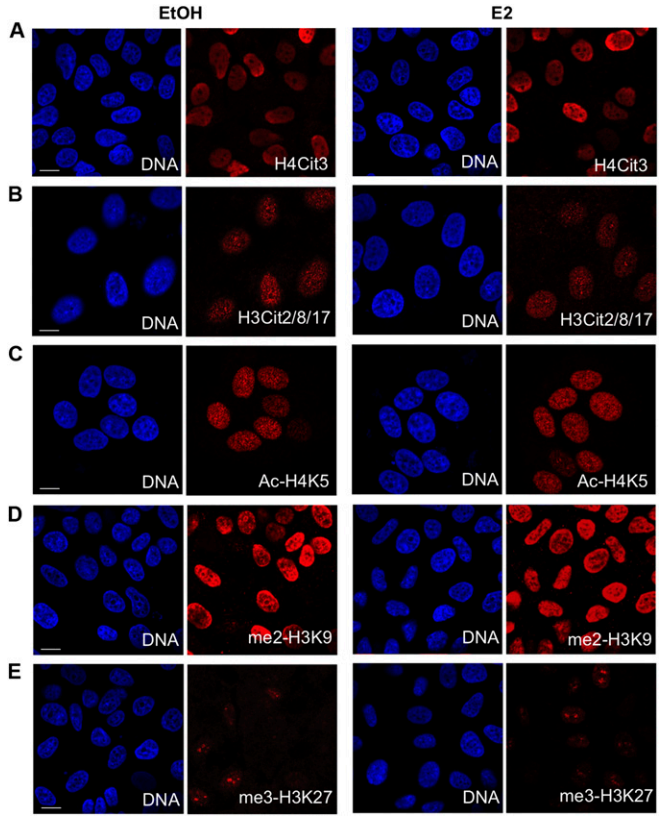

Fig. S2. Estrogen treatment does not appear to globally affect levels of other histone modifications in MCF-7 cells. Confocal immunofluorescence images show that the signals for H4Cit3 (*A*), H3Cit2/8/17 (*B*), Ac-H4K5 (*C*), me2-H3K9 (*D*), and me3-H3K27 (*E*) signals do not appear to change after E2 stimulation. (Scale bars: 10 μm.)

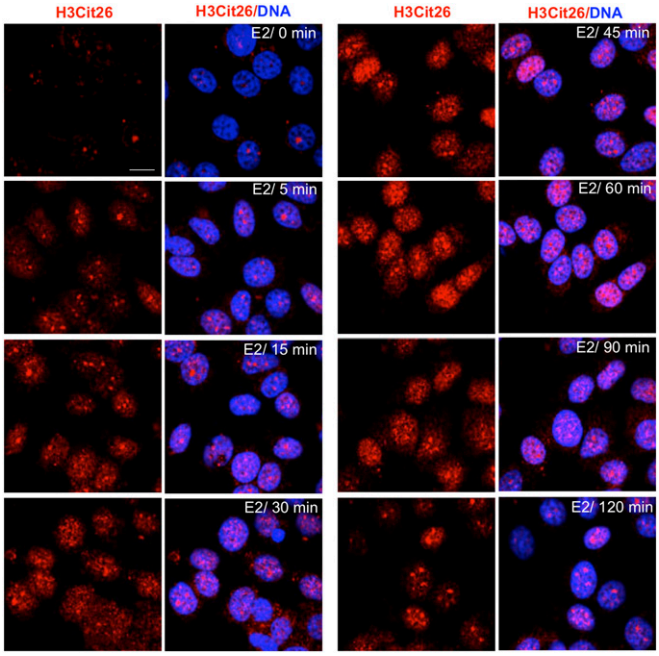

Fig. S3. Time course of E2-induced global H3R26 citrullination in MCF-7 cells. Confocal immunofluorescence microscopic images showing that treatment of estrogen-starved MCF-7 cells with 100 nM of E2 results in H3R26 citrullination within 5 min and that the signal peaked at 45 min after E2 treatment. (Scale bar: 10 μm.)

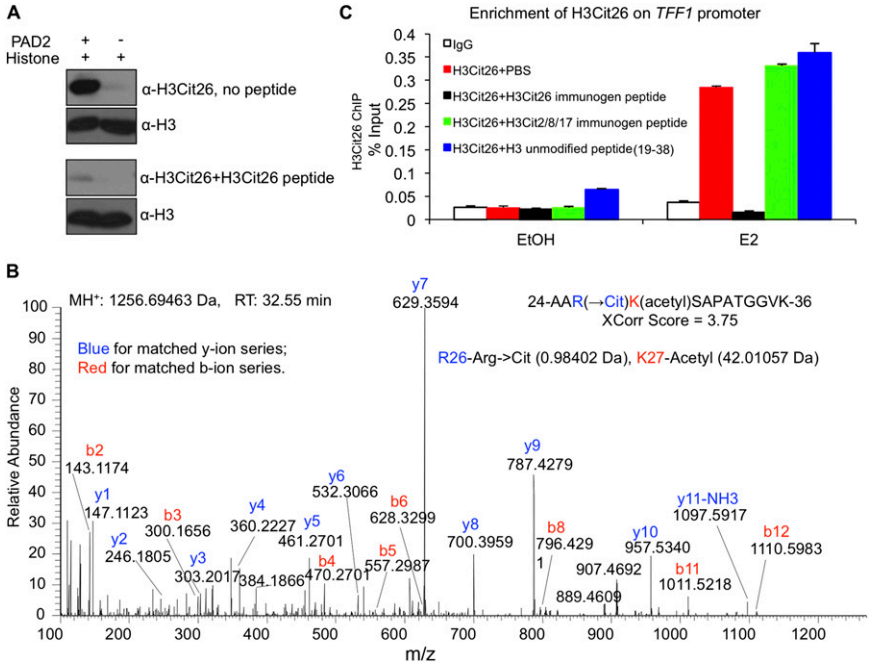

Fig. S4. H3Cit26 antibody specificity. (*A*) Specificity of the anti-H3Cit26 antibody was tested with peptide competition assay. Western blot showing that the anti-H3Cit26 antibody is specifically reactive with the appropriately sized band from human PAD2-treated MCF-7 cell histones but not from nontreated histones. Anti-H3Cit26 antibody was preincubated with 1 μg/mL H3Cit26 immunogen peptide (Abcam; ab20631) overnight at 4 °C before Western blot analysis. The competing peptide nearly completely blocked detection of H3Cit26. Anti-histone H3 staining revealed the presence of approximately equal amounts of histone in each lane. (*B*) The positive band in *A* was subjected to MS/MS analysis. Citrullination at R26 of the tryptic peptide AARKSAPATGGVK from human histone 3 was detected by nanoLC-MS/MS analysis. MS/MS spectrum of the doubly charged peptide ions at *m/z* $[628.8510]^{2+}$ with elution time at 32.55 min shows almost all y-ion series and b-ion series, demonstrating that R26 residue was converted to Citrulline (Arg > Cit) with increased 0.98402 Da. Meanwhile, K27 was identified as being acetylated (42.01057 Da). The MS/MS spectrum was searched against human database by using Proteome Discoverer 1.2 software with integrated SEQUEST searching engine with XCorr:3.75, and Probability:51.10. (*C*) ChIP analysis showing that H3Cit26 enrichment on TFF1 promoter is specifically competed by the H3Cit26 immunogen peptide. Anti-H3Cit26 antibody was mock- (PBS incubation) or preincubated with 1 μg/mL H3Cit26 immunogen peptide (Abcam; ab20631), H3Cit2/8/17 immunogen peptide (Abcam; ab32876), or unmodified histone H3 (19–38) overnight at 4 °C. IgG was used as a control.

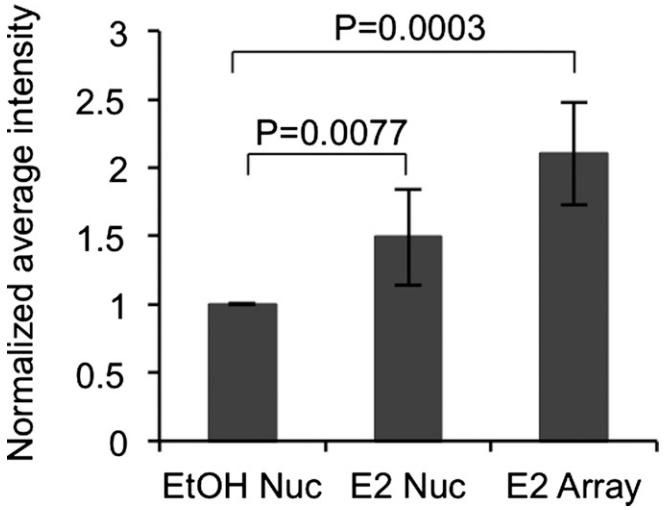

Fig. S5. Quantitation of H3Cit26 at the PRL-array. The histogram shows relative intensity for the anti-H3Cit26 signal in E2-treated nucleoplasm (E2 Nuc) and E2-treated array (E2 Array) compared with EtOH treated nucleoplasm (EtOH Nuc). *P* values were calculated based on the basis of two-tailed Student *t* test.

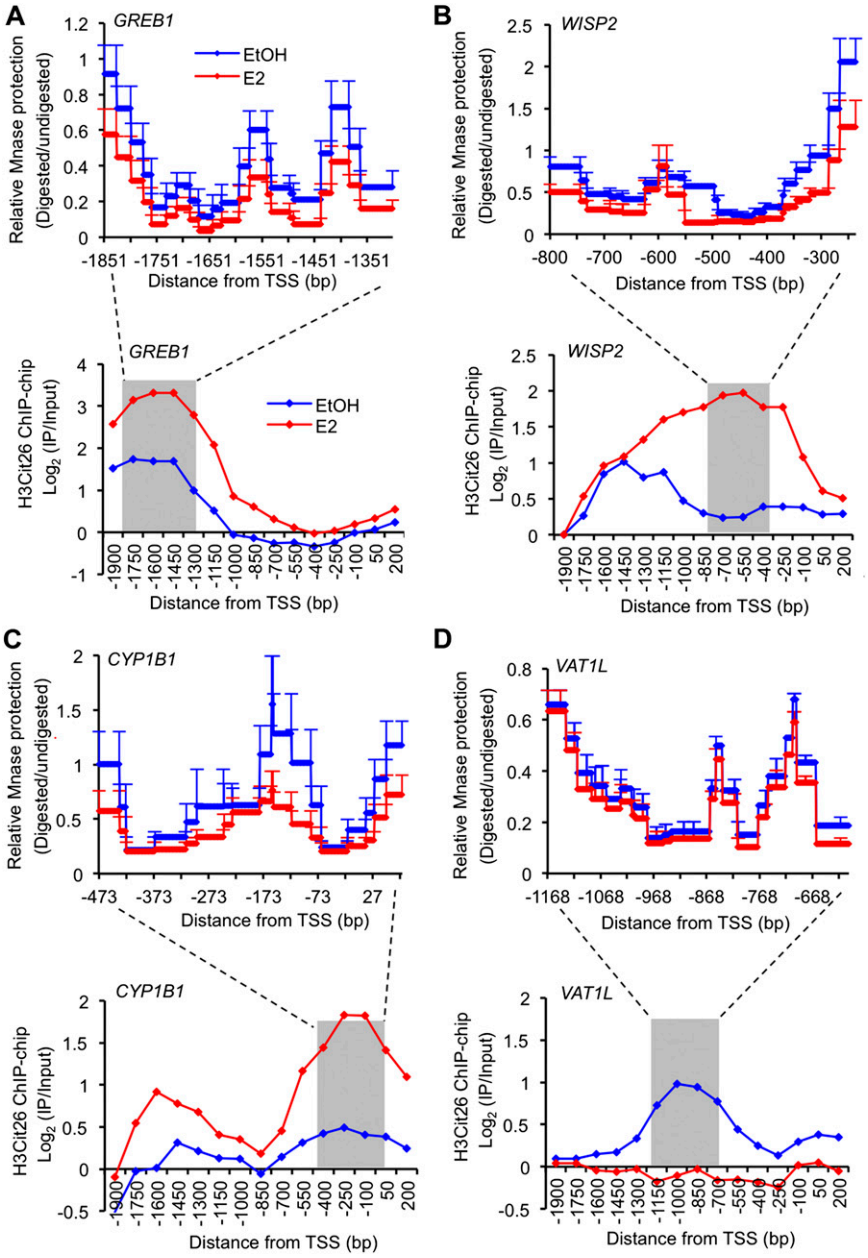

Fig. S6. After estrogen stimulation, H3R26 citrullinaton facilitates an open chromatin architecture at the EREs of E2-induced gene promoters. In each graph, GREB1 (*A*), WISP2 (*B*), CYP1B1 (*C*), or VAT1L (*D*), *Upper* shows the MNase protection assay following EtOH or E2 treatment in MCF-7 cells. qPCR was performed to tile through the proximal promoter ERE region with overlapping amplicons (~100-bp PCR product average, with ~20-bp overlap). Relative ratio of the amount of digested DNA to genomic control was used to determine the extent of MNase protection. Values from overlapping primer sets are averaged. Each point represents the mean + SEM, $n = 3$. *Lower* shows the H3Cit26 ChIP-chip signal at the proximal promoter ERE region of E2-induced target.

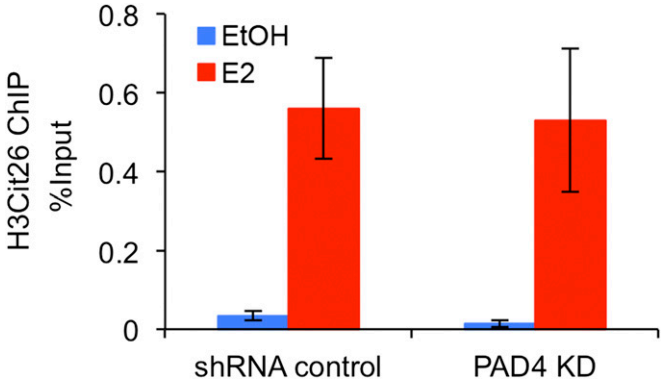

Fig. S7. Depletion of PAD4 does not inhibit H3Cit26 enrichment on *TFF1* ERE region. Depletion of PAD4 (PAD4 KD) from MCF-7 cells was described (3). E2 treatment induced the pronounced enrichment of H3Cit26 on the *TFF1* ERE region in the shRNA control MCF-7 cells, whereas this increase was not observed in the PAD4 depleted line.

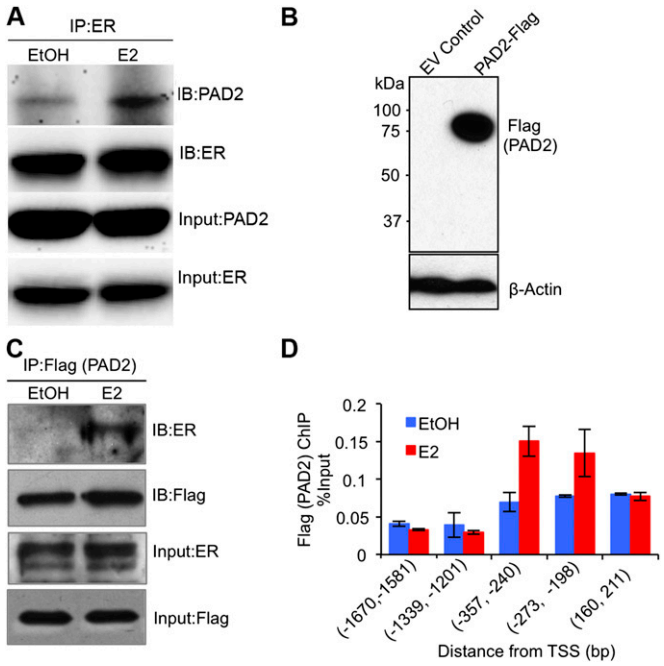

Fig. S8. E2 stimulates the association of PAD2 with ER at the ERE region on the *TFF1*. (*A*) Coimmunoprecipitation analysis in wild-type MCF-7 cells reveals that E2 treatment stimulates the interaction between endogenous PAD2 and ER. (*B*) Western blotting documenting PAD2 overexpression. EV represents the empty vector control. β-actin (*Lower*) revealed equal protein loading. (*C*) Coimmunoprecipitation analysis of MCF-7 cells stably overexpressing Flag-PAD2 reveals that E2 treatment stimulates the interaction between endogenous ER and ectopically expressed PAD2. (*D*) Ectogenic PAD2 is recruited to TFF1 ERE promoter region after E2 treatment. ChIP assay with anti-Flag antibody on the TFF1 tilling promoter regions in the MCF-7 cells stably overexpressing PAD2. E2 stimulation induced PAD2 recruitment to the ERE region.

Table S1. Steady-state kinetic parameters for histone H3 and H4 substrates

Enzyme	Substrate	k_{cat}, s^{-1}	K_m, mM	k_{cat}/K_m, $s^{-1}\cdot M^{-1}$
PAD2	H3	ND*	ND*	1,200
	H3 (1–15)	2.4 + 0.10	1.9 + 0.25	1,250
	H3 (22–30)	1.4 + 0.17	3.7 + 1.0	370
	H4	ND*	ND*	2,400
	H4 (1–15)	1.4 + 0.1	1.0 + 0.2	1,400
PAD4	H3	ND*	ND*	3,700[†]
	H3 (1–15)	0.6 + 0.03	3.3 + 0.4	180
	H3 (22–30)	ND*	ND*	60
	H4	1.2 + 0.2[‡]	0.1 + 0.03[‡]	9,000[‡]
	H4 (1–15)	2.5 + 0.1	0.6 + 0.1	4,400

Kinetic parameters were measured by incubating the enzyme at 37 °C.
*ND, not determined due to a lack of saturation in the *v* versus [S] curves.
[†]Value taken from ref. 1.
[‡]Value taken from ref. 2.

1. Slack JL, Causey CP, Luo Y, Thompson PR (2011) Development and use of clickable activity based protein profiling agents for protein arginine deiminase 4. *ACS Chem Biol* 6:466–476.
2. Knuckley B, et al. (2010) Substrate specificity and kinetic studies of PADs 1, 3, and 4 identify potent and selective inhibitors of protein arginine deiminase 3. *Biochemistry* 49:4852–4863.

Table S2. ERE matrix file found by MEME from the 208 E2-induced H3Cit26 binding sites

Position	"A"	"C"	"G "	"T"
1	0.048780	0.000000	0.658537	0.292683
2	0.000000	0.073171	0.926829	0.000000
3	0.000000	0.000000	0.000000	1.000000
4	0.000000	1.000000	0.000000	0.000000
5	1.000000	0.000000	0.000000	0.000000
6	0.073171	0.585366	0.341463	0.000000
7	0.414634	0.292683	0.121951	0.170732
8	0.000000	0.341463	0.487805	0.170732
9	0.146341	0.000000	0.000000	0.853659
10	0.073171	0.195122	0.682927	0.048780
11	0.243902	0.170732	0.292683	0.292683
12	0.170732	0.829268	0.000000	0.000000
13	0.000000	0.634146	0.000000	0.365854
14	0.097561	0.121951	0.097561	0.682927
15	0.024390	0.243902	0.243902	0.487805